Diamond Detectors for Radiation and Luminosity Measurements in CMS

R. Hall-Wilton *CERN,* M. Pernicka *HEPHY Vienna* E. Bartz, J. Doroshenko, D. Hits,S. Schnetzer, R. Stone, *Rutgers University,* V. Halyo, B. Harrop, A. Hunt, D. Marlow, *Princeton University,* W. Bugg, M. Hollingsworth, S. Spanier, *University of Tennessee,* W. Johns, *Vanderbilt University*

***Abstract*—The Beam Conditions Monitor (BCM) provides fast, relative measurements of particle fluxes for use in the safety systems of CMS. It uses a set of Chemical Vapor Deposited (CVD) diamond diodes. Sudden, order of magnitude changes in the BCM readout issue non-maskable LHC beam aborts. Dangerous irradiation trends on longer timescales translate into automatic detector interlocks and injection inhibit. Operators in the LHC beam and CMS detector control room obtain and display real time (1Hz) readout of flux measurements from the BCM subsystem. The beam radiation monitoring system also provides an independent measurement of the beam luminosity. The next generation luminosity detector, called the Pixel Luminosity Telescope (PLT), is based on pixelated monocrystalline diamond detectors. They provide a fast occupancy information and allow particle tracking near the interaction point to distinguish trajectories originating from the proton-proton collision point and those parallel to the beam pipe. We present the use case of diamond detectors for beam radiation monitoring in CMS and first measurements of 150 GeV/c π^+ particle tracks in three layers of pixelated diamond detectors. The PLT after installation in 2010 will be the largest utilization of diamond instrumentation in High Energy Physics.**

I. Introduction

THE LHC will expose CMS to radiation levels as high as 2×10^{14} protons/cm^2 at the location of the innermost silicon pixel layer (distance to beam $r = 4$ cm). The silicon detectors of CMS are designed to withstand the radiation at the highest luminosity for a time of three years. Under adverse beam conditions with higher radiation levels the lifetime of instruments is reduced, or they can be damaged. It is therefore important to measure the particle flux in order to provide instrument protection via interlocks, issue fast beam aborts, and to provide monitoring data for shifters to establish safe beam conditions over time. To achieve these goals, the Beam Radiation Monitoring (BRM) group has installed multiple instruments along the beam pipe that measure the particle flux in CMS [1]: two Beam Conditions Monitor systems (BCM1/2) and Beam Scintillator Counters (BSC). Each of these instruments provides live displays ($\approx$ 1 Hz update rates) to CMS, LHC, and FNAL, as well as archived data for comprehensive analyses. The instrument which is closest to the silicon pixel detector is the BCM1L. It utilizes 4+4 polycrystalline CVD diamond diodes with an active area of 10 mm $\times$ 10 mm $\times$ 0.4 mm to measure particle flux. If the particle flux exceeds preset thresholds, it provides warning and abort signals to both LHC and CMS. The next detector to be added into the BRM system is the PLT, which will specialize in luminosity measurements, in addition to radiation measurements.

Speaker and contact: hollings@cern.ch

II. Pixel Luminosity Telescope

The PLT is a dedicated luminosity monitor for CMS based on monocrystalline CVD diamond pixel sensors. It is designed to provide a high-precision measurement of the bunch-by-bunch relative luminosity at the CMS collision point on a time scale of a few seconds and a stable high-precision measurement of the integrated relative luminosity over the entire lifetime of the CMS experiment [3]. The PLT consists of two arrays of eight small-angle telescopes situated one on each end of CMS. Figure 1 shows a three dimensional design drawing of a PLT array. The telescopes consist of three equally-spaced planes of diamond pixel sensors with a total telescope length of 7.5 cm. They are located about 5 cm radially from the beam line at a distance of 1.8 m from the central collision point. Each telescope will be projective at an angle of 1.56° to the interaction point corresponding to a rapidity of $\eta = 4.3$.

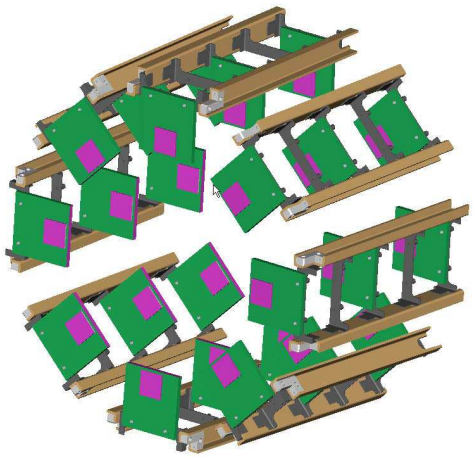

Fig. 1. 3D design drawing of the telescope array at one side of the CMS detector, with the beam pipe in its center not shown. The distance between two outer detector planes is 7.5 cm.

III. Monocrystalline Diamond Detector

Diamond sensors are crucial for the PLT application since they will operate efficiently with only moderate decrease

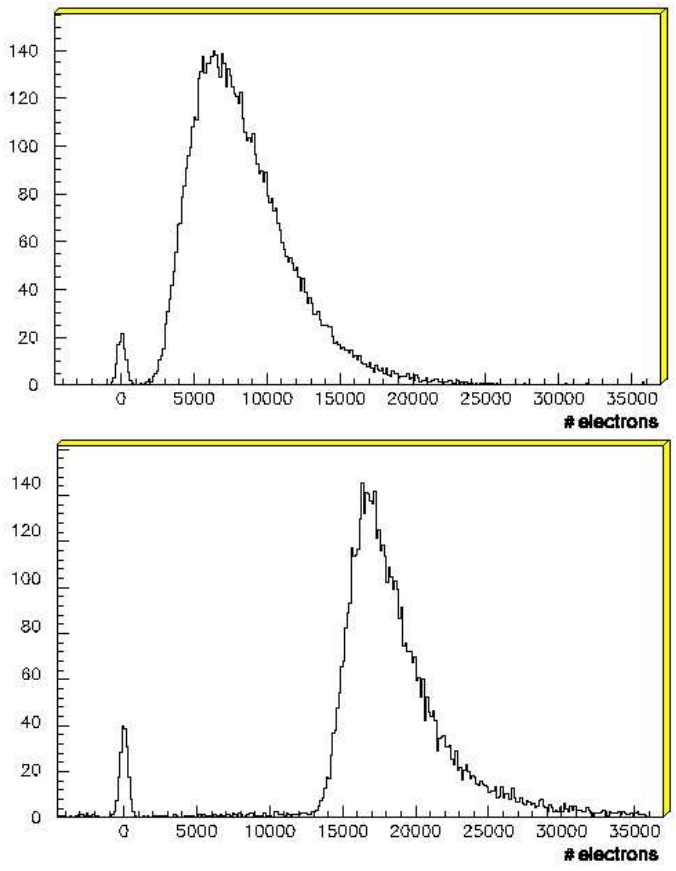

Fig. 2. Charge deposit distributions for electrons from a ^{90}Sr source in polycrystaline CVD diamond (top) and monocrystalline CVD diamond (bottom).

in signal size over the entire lifetime of CMS [4]; they are capable of surviving up to 2×10^{15} protons/cm^2. Of equal importance, this radiation hardness does not require that the sensors be cooled. Furthermore, full charge collection is achieved with an electric field between 0.2 V/μm and 0.4 V/μm. Monocrystalline diamond is used for the sensor material rather than polycrystalline diamond since the pulse height distribution of monocrystalline diamond is large and well separated from zero, ensuring that any efficiency changes due to threshold drifts will be small. A comparison of the charge collection properties for both types of diamond is shown in Fig. 2.

IV. Detector Readout

The telescope planes consist of monocrystalline diamond sensors. Each sensor is configured with a pixel pattern electrode and bump bonded to the PSI46v2 CMS pixel readout chip [2]. The reason for using pixels is to reduce the capacitance of each channel and, thereby, the inherent serial noise so that the sensor can be read out in the bunch crossing time of 25 ns. Furthermore, it allows to measure tracks for high precision detector alignment and to re-define the active area by masking individual pixels. A schematic drawing of a fully constructed sensor is shown in Fig. 3.

Deposition of the pixel electrode pattern on the diamonds and the bump-bonding of the diamond sensors to the pixel readout chips were performed at the Princeton Institute of Science and Technology Materials (PRISM) micro-fabrication laboratory. Following surface preparation, electrodes were sputtered onto the diamond surface using a Ti/W alloy target as an under bump metalization (UBM). A 4 mm$\times$4 mm electrode was deposited on one side of the diamond using a shadow mask. On the other side, a pixel pattern was deposited using a standard lift-off photolithographic process. The pattern covered an area of 3.9 mm$\times$4.0 mm and consisted of an array of 26 $\times$ 40 pixels with pitch of 150 μm $\times$ 100 μm matching that of the PSI46v2 chip.

The PSI46v2 chip features individual pixel threshold/mask settings, full analog readout of the pixel hit address and charge deposit, as well as a column-multiplicity signal (known as the fast-or), which indicates the number of double columns that had pixels over threshold in each bunch crossing. The primary luminosity measurement of the PLT is based on counting the number of telescopes with three-fold coincidences formed from the fast-or output. Fast-or signals are read at bunch-crossing rate of about 40 MHz, while the full pixel information, consisting of the row and column addresses and the pulse heights of all pixels over threshold, is read out at a lower rate of a few kHz. The full pixel readout provides tracking information and is a powerful tool for determining systematic corrections, calibrating pixel efficiencies and measuring the real-time location of the collision point centroid.

The detector readout is done in the same manner as for the CMS silicon pixel detectors, which includes a Front End Driver (FED) and Front End Controller (FEC) [5]. The signals for each telescope plane will be sent over standard CMS optical fiber analog links to the electronics room where a three-fold coincidence for each telescope will be formed.

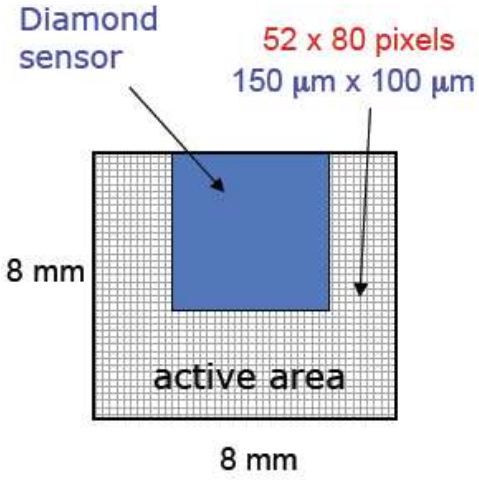

Fig. 3. A schematic drawing of the diamond detector as placed on the CMS pixel readout chip.

V. Beam Test of the PLT

In order to determine the performance of the diamond pixel sensors and the robustness of the PLT design, we carried out a test of a prototype telescope in a 150 GeV/c π^+ beam in the H4 beam line of the CERN SPS in May of 2009. The

primary goals of this test were to determine: the yield of good pixel channels that result from the bump-bonding process, the pulse height response of the diamond sensors for minimum ionizing particles, the fast-or signal efficiency, and the tracking capability of the diamond pixel planes. With 48 hours of beam time, we were able to complete the core components of the program.

A. Setup and Preparation

Figures 4 and 5 show a fully assembled telescope and the setup in the beam line, respectively. Small scintillators, each with an area 8 mm$\times$8 mm perpendicular to the beam (see Fig. 5), were positioned just upstream and downstream of the telescope. All of the results reported here are based on events triggered by a coincidence of these two scintillators, although the PLT will ultimately be self-triggered through fast-or coincidences. When a trigger coincidence occurred a signal was sent to the FED via a CMS Timing Trigger and Control Interface (TTCci) module initiating digitization. In order to have a wide time view of the event, the digitization started three clock periods before the event and continued for 960 clock periods.

The telescope planes were calibrated using the built-in pulsing capability of the PSI46v2 readout chip. Internally the readout chip can be programmed to deposit known amounts of charges into selected pixel channels. For each individual pixel repeatedly different amounts of charges in the full readout range were injected and readout via the FED. The input charge as function of the FED was described by a second-order polynomial to obtain a mapping from ADC count to pulse height in number of electrons.

Before taking data, a procedure, similar to that for the CMS pixel detectors, was used to lower the pixel thresholds as much as possible [6]. This multiple-step procedure involved adjusting three parameters in the readout chip: the overall course threshold, the trimming range around this setting and the trimmed threshold for each individual pixel. The pixel thresholds achieved were in the range of 2,500 to 4,500 electrons.

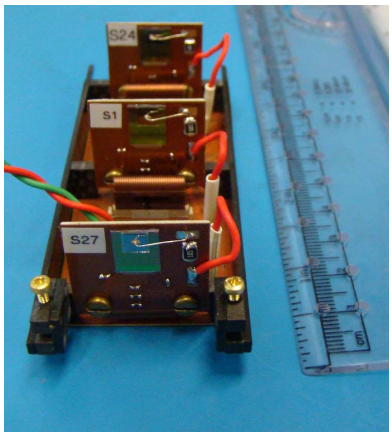

Fig. 4. Front view of the fully assembled PLT telescope used in the test beam.

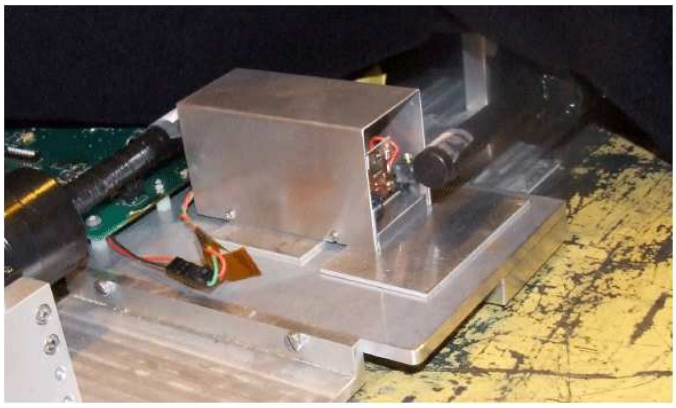

Fig. 5. Test beam setup of telescope inside metal housing with upstream (right side) and downstream (left side) trigger scintillators.

B. Occupancy

Figure 6 shows coincident hits in the telescope planes. The first five columns of plane 1 were disabled because of bonding problems caused by the wedge shape of this sensor. Due to several noisy pixels, the rightmost column of plane 1 was also disabled. All of the rest of the columns in all three planes were enabled. In all three planes, pixels in the upper extreme row tend to have a larger number of hits than other rows. This is not currently understood but may be related to the fact that the diamond is mounted close to the edge of the readout chip. This row and six noisy pixels in plane 1 were masked off for all subsequent analyses.

Except for the disabled columns, nearly all pixels were active. The number of pixels without any hits are 1.8%, 2.2% and 0.1% for planes 1, 2 and 3, respectively, indicating, that for these planes the yield of good pixel bump connections was 98% or better. Since the time that these sensors were bump-bonded, we have continued to improve and gain experience with the process and expect that the current percentage yield of good bump connections is even higher.

C. Charge Deposit

For determining charge deposit distributions, we defined an acceptance region in each of the three planes such that if a beam particle were incident on this region in two of the planes it was certain to also be incident on the enabled area of the third plane. Because the telescope was at a slight upward angle with respect to the beam, there was an approximately 8 row offset between planes 1 and 3 in particle hit position. Figure 7 shows an example of the summed charge distribution in units of collected electrons. We also required that there be one and only one cluster in each plane. The pulse height plotted is the sum over all pixels within the hit cluster. We found that the most probable signal is approximately 16,000 electrons for plane 1 and approximately 18,500 electrons for planes 2 and 3. There is a 10% systematic uncertainty in calibration from plane to plane. The most probable pulse height in plane 1 is about 15% lower than that for planes 2 and 3. This is largely due to the fact that the average thickness of the diamond sensor for this plane was less than that of the other two; planes 2

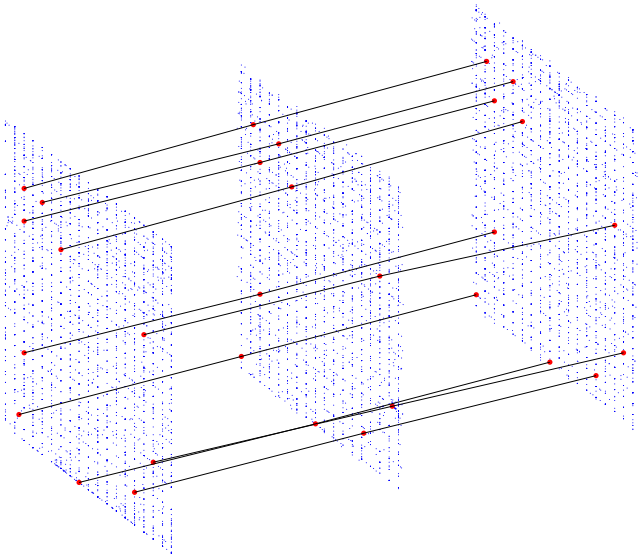

Fig. 6. 3D display of pixel occupancies. For demonstration purpose, the lines connect a small subset of hits that were in coincidence. Due to the nearly perpendicular incidence of the particles on the detector planes for most of the tracks we obtain single pixel hits (no charge sharing). In this case, the corresponding hit position is assumed in the center of the pixel. For charge deposits in neighboring pixels we calculate the charge weighted average position amongst them.

and 3 were 499 μm and 496 μm thick, respectively while plane 1 was wedge-shaped and had an average thickness of 457 μm with a variation of 50 μm from one side to the other. For comparison, the most probable signal for a 300 μm thick silicon sensor is 22,000 electrons.

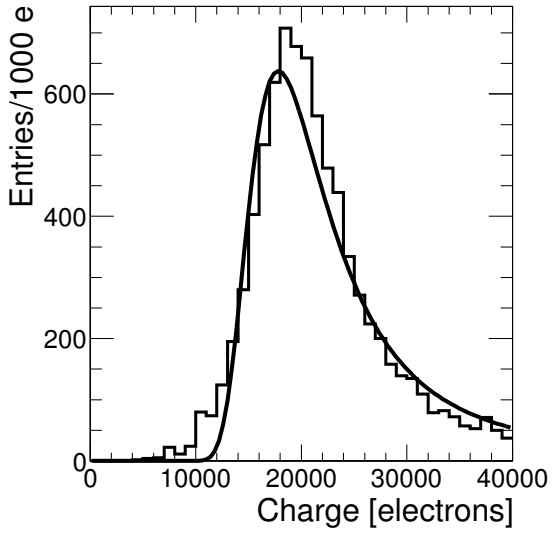

Fig. 7. Summed charge distribution for plane 3. The solid line represents the best fit to a Landau distribution.

We can obtain a measure of the pixel threshold settings by examining the turn on of the distribution for low pulse heights. Most of the low charge signals per pixel result from charge sharing when the particle hits close to a pixel boundary. These distributions indicate that the threshold turn on is 3,500 to 4,500 electrons, 3,000 to 4,000 electrons and 2,500 to 3,500 electrons for planes 1, 2 and 3, respectively. Although these thresholds are already low, if there had been more time to tune and iterate the threshold trimming lower values could likely have been achieved.

D. Tracking and Alignment

In order to reconstruct tracks in the telescope, we first found the clusters associated with particle hits in each plane. Pixels above threshold that were nearest neighbors in either the row or column direction were merged. On average, about 70% of the events had one hit per cluster, 25% had two hits per cluster, and 5% had more than two hits per cluster. For our analysis, we excluded clusters in which three or more pixels were aligned in either a row or column. The resulting clusters consisted of one, two, three or four nearest neighbor pixels. The cluster position was calculated as the average of the positions of its constituent pixels weighted by their collected charge. Figure 6 shows a sample of tracks in a three-dimensional display. For this plot, events were selected in which there was one and only one cluster in each of the three planes. Events of this type constitute 89% of all events.

We define the residual of the track in the coordinate x where x measures along the 150 μm side of the pixels, as $\Delta x = x_2 - \frac{x_3 - x_1}{2}$. The x_1, x_2, and x_3 are the cluster hit positions in plane 1, 2, and 3, respectively. We define Δy correspondingly. The indices are interchanged to iterate the reference planes. The residual above can be used to measure the relative offset of plane 2 with respect to planes 1 and 3. As shown in Fig. 8, this offset is $\Delta x = 25$ μm ± 5 μm in the column direction (used 57 tracks) and $\Delta y = 146 \mu$m $\pm$ 3 μm in the row direction (used 140 tracks). Even though this is based on a few tracks, only, the alignment was achieved to a high precision. The accuracy depends on the positioning of detectors onto the telescope planes, and of the planes into the telescope during the assembly process. The accuracy is well within the requirements for the PLT.

E. Fast-Or Efficiencies

The fast-or signals form the basis for the primary luminosity measurement of the PLT. Synchronized with the LHC bunch crossing rate of about 40 MHz, they will allow the three-fold coincidence rate within each telescope to be formed for each LHC bunch crossing, thereby determining the relative bunch-by-bunch luminosity. Understanding these fast-or signals and measuring their efficiency is key to establishing the performance of the PLT. While the fast-or output of the PSI46v2 chip was implemented for possible application in the Level-1 trigger, the results presented here are the first systematic efficiency studies.

For determining the fast-or efficiencies, we imposed the same requirements as for the pulse height measurement above in order to ensure that a particle passed through the enabled area of the plane under test. Single clusters were required in each of the three planes and, for the two planes other than the one under test, the cluster positions were required to be in the previously described fiducial regions. In the test beam, the arrival time of beam particles was uncorrelated with the

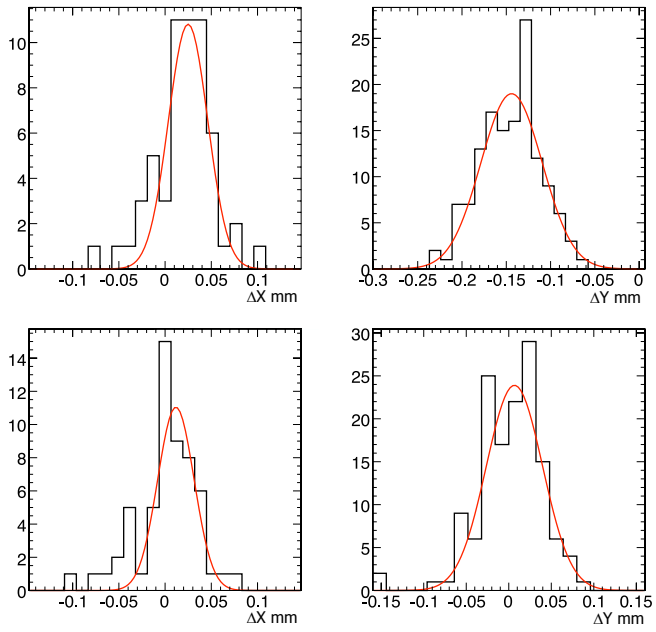

Fig. 8. Residuals for tracks with more than two hits per cluster, before (upper row) and after (lower row) alignment.

clock phase. Due to time walk, a particle that arrived shortly after the leading clock edge and that had a large pulse height might be output one clock period earlier than the clock time of the trigger. Similarly, a particle that arrived shortly before the trailing clock edge and that had a small pulse height might be output one clock period later than the clock time of the trigger.

For the PLT running at the LHC, the clock will be synchronized with the bunch crossing and particle arrival times will be fixed to within a few nanoseconds relative to the clock edge. The clock phase at the readout chips can then be adjusted so that all of the fast-or signals will occur in the "'in-time"' clock pulse. In order to correctly determine the fast-or efficiency using the test beam data, it is necessary to count fast-or signals that occur one clock period early or one clock period late as well as those that occur in-time. The correction due to accidental firing of the fast-or signal was found to be negligible: in the nine clock pulses occurring between 2.50 μs and 2.75 μs after a triggered event, there were 87 fast-or signals out of 100,000 events giving a 0.03% probability for an accidental fast-or in a three clock period. The measured efficiencies are 99.3% for plane 1, 99.6% for plane 2, and 99.9% for plane 3.

VI. Conclusions

The CMS detector at LHC extensively uses CVD diamond detectors to monitor and act on adverse beam conditions. As a new addition, the PLT will also provide bunch-by-bunch luminosity measurements at a required relative systematic uncertainty of about 1%. To achieve this it utilizes pixelated monocrystalline CVD diamond detectors. We have completed a preliminary analysis of data from a test of a prototype PLT telescope in a high-energy pion beam. The fraction of active pixel channels in all three planes is 98% or more. The most probable value in the measured pulse height distribution for 150 GeV pions from the SPS at CERN is about 18,000 electrons for a 500 μm thick detector. This is well above the average pixel threshold setting of 2,500 to 4,500 electrons. The efficiency of the fast-or signals that form the basis of the luminosity measurement is greater than 99% for all three planes. Clear and well defined tracks are readily reconstructed in the telescope and allow high precision detector alignments.

The full version of the PLT (2 modules$\times$8 telescopes$\times$3 layers of diamond pixel detectors) is now projected for installation during the Fall 2010 shutdown of LHC.

Acknowledgment

We thank the following people for their contributions to the PLT project: A. Butler, P. Butler ,and N. Rodrigues from Canterbury University; V. Ryjov from CERN; L. Lueking from Fermilab; S. Schmid and H. Steininger from HEPHY Vienna; Y. Gershtein, E. Halkiadakis, and A. Lath from Rutgers University; B. Sands and D. Stickland from Princeton University; R. Lander from University of California, Davis; and B. Gabela from Vanderbilt University. We also thank the CERN SPS accelerator group for their excellent operation and support.

References

[1] Bell, Alan. J., "Beam & Radiation Monitoring for CMS," Nuclear Science Symposium Conference Record, 2008. NSS '08. IEEE , vol., no., pp.2322-2325, 19-25 Oct. (2008).
[2] M. Barbero *et al.*, "Design and test of the CMS pixel readout chip," Nucl. Instrum. Meth. A 517, 349 (2004).
[3] E. Halkiadakis, Nucl. Instrum. Meth. A 565, 284 (2006).
[4] W. Adams *et al.*, "Radiation hard diamond sensors for future tracking applications," Nucl. Instrum. Meth. A 565, 278 (2006).
[5] D. Kotlinski *et al.*, "The control and readout systems of the CMS pixel barrel detector," Nucl. Instrum. Meth. A 565, 73 (2006); C. Foudas *et al.*, IEEE Trans. Nucl. Sci. 52, 2836 (2005).
[6] D. Kotlinski, "Status of the CMS Pixel detector," J. Instrum. 4, P03019 (2009).